Direct synthesis of self-aligned single-walled carbon nanotubes on paper

5 authors, including:

Qin Zhou
University of California, Berkeley
30 PUBLICATIONS **497** CITATIONS

Shaomin Xiong
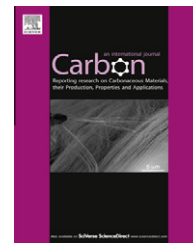University of California, Berkeley
23 PUBLICATIONS **230** CITATIONS

Direct synthesis of self-aligned single-walled carbon nanotubes on paper

Qin Zhou [a,*], Kaihui Liu [b], Shaomin Xiong [c], Feng Wang [b], Liwei Lin [a]

[a] Berkeley Sensor and Actuator Center, Department of Mechanical Engineering, University of California, Berkeley, CA 94720, USA
[b] Department of Physics, University of California, Berkeley, CA 94720, USA
[c] Department of Mechanical Engineering, University of California, Berkeley, CA 94720, USA

ARTICLE INFO

ABSTRACT

A technique of micro chemical vapor deposition (μCVD) is reported for the direct synthesis of self-aligned SWCNTs on various substrates including plastics and paper. With the guidance of micro flow channels, self-aligned SWCNTs up to hundreds of microns in length have been collected. Both Raman spectral and transmission electron microscopy have validated the high quality of these SWCNTs. In conclusion, μCVD could be a versatile method to synthesize pristine SWCNTs for various applications.

Published by Elsevier Ltd.

1. Introduction

The integration of nanomaterials with flexible substrates has drawn great interests targeting low-cost and lightweight applications [1–5]. Among various nanomaterials, single-walled carbon nanotubes (SWCNTs) have a unique set of specific properties including high electronic mobility [6], high electrical current carrying capability [7,8], and ballistic electron transport phenomenon at room temperature [9,10]. These breakthrough demonstrations of SWCNTs, however, have all been based on the direct growth of SWCNTs in high temperature chambers without post-assembly processes to avoid possible degradations during the transfer processes [11–19]. Specifically, two types of transfer processes have been commonly employed for one-dimensional nanostructures. The solution-cast approach starts with the dispersion of SWCNTs with liquid to form a nanotube ink, which is later deposited onto a target substrate and dried [14–18]. Nanotubes deposited by this method usually exhibit degraded electrical performance due to random alignment [15,18], ultrasonic agitation [20], and/or electrical property modifications from the SWCNT–solvent interactions [21,22]. The second approach starts with the synthesis of well-aligned SWCNTs with the aid of electrical field [23], gas

flow [24,25], or crystal lattice orientation on the growth substrate [26]. Afterwards, a transfer layer (usually polymer) is deposited and SWCNTs are attached to the transfer layer and relocated to a target substrate [27,28]. The transfer layer is later dissolved or etched away, leaving aligned SWCNTs on the target substrate. This approach preserves the originally well-aligned patterns but various chemicals used in the process could affect the electrical properties of SWCNTs due to chemical doping and surface adsorption [21]. Here we describe a different approach without the transfer process to allow as-grown SWCNTs to be directly placed onto arbitrary substrates with self-aligned patterns such as glass, ceramics and temperature-sensitive substrates including plastics and papers.

2. Experimental

2.1. Concept and setup

Fig. 1 illustrates the basic principle and the setup of the synthesis process. Briefly, micro chemical vapor deposition (μCVD) system which is part of the suspended cantilever microstructure [29], is built by means of silicon micromachining processes. Adequate heat transfer design limits the high
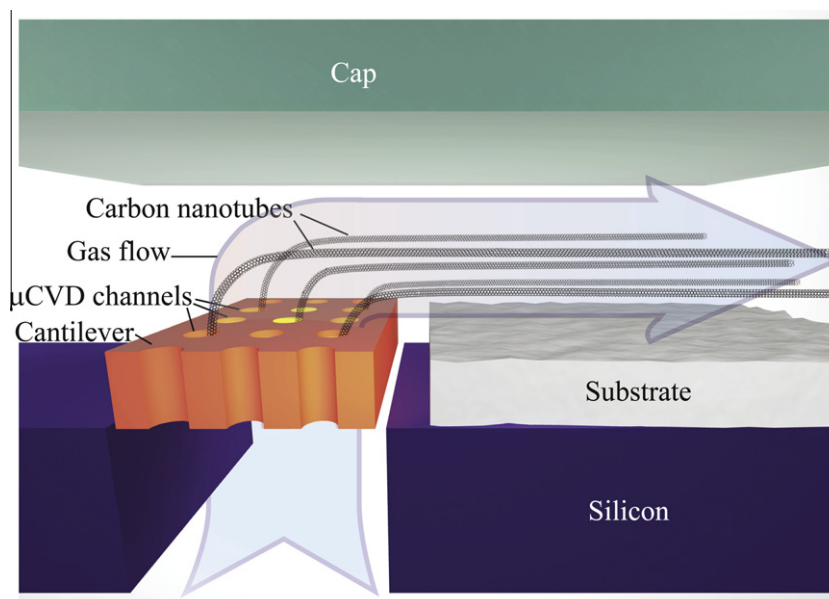

Fig. 1 – Schematic diagram illustrating the direct synthesis of self-aligned SWCNTs onto an arbitrary substrate. Nanotubes are synthesized from the μCVD channels at high temperature. The high-temperature region is localized at the suspended cantilever to allow a temperature sensitive substrate to be placed nearby. The gap between the cap and the substrate creates a micro gas flow channel which ensures laminar flow condition. This laminar gas flow guides the growth of nanotubes so that they stay straight and well-aligned. The nanotubes are deposited onto the substrate after the gas flow is turned off.

temperature region to be localized on the cantilever. As such, temperature sensitive target substrate can be placed close to the cantilever without experiencing high temperature damages from the synthesis process. The gap between the top "cap" and bottom μCVD chip forms a narrow gas channel which guides the growth direction of SWCNTs over the nearby target substrate. The narrow gas channel also reduces Reynolds number and avoids turbulent flow, which is desirable in this case to effectively guide and align the synthesized SWCNTs. This steady laminar flow also ensures that the floating nanotubes do not get contact with the substrates during the growth. The gas flow is initiated by applying a pressure difference between the bottom of the μCVD chip and the outside environment. The magnitude of this pressure difference determines the overall flow velocity; while the configuration of the flow channels determines the flow pattern. A detailed simulation is done to support this flow pattern and can be found in the Supplementary material. At the end of the growth process, the heating power and the gas are turned off to allow the SWCNTs to be deposited onto the target substrate.

2.2. Design of the microheater

The high temperature region for the synthesis process is near the tip of the U-shaped micro cantilever as illustrated in Fig. 2a. The heating power is generated by joule heating when an electrical current is applied. The highest temperature is at the tip of cantilever since majority of heat will dissipate via heat conduction through the two anchors to the silicon substrate. In the prototype design, four μCVD units have been constructed on a chip of $6 \times 5\ mm^2$ in size as shown in the optical image in Fig. 2b. When the electrical power is applied

to the second μCVD unit from the left, the micro-heater is observed to glow visibly at high temperature. The corresponding infrared image in Fig. 2c (FLIR® A320 Camera, the emissivity of the μCVD chip surface is calibrated to be 0.75. See Supplementary data) validates that the high temperature region is localized at the micro-heater. Materials that cannot sustain high temperature can therefore be placed close to the micro-heater unit without thermal damages or degradations during the synthesis process. For example, a 50-μm-thick sticky tape (Kapton®, 2 mil) as seen at the bottom of Fig. 2b has been used as the spacer to adjust the height of the gas flow channel between the top cap and the μCVD unit and no visible damages have been identified after the growth process.

The cantilever design causes non-uniform temperature distribution along its length which could potentially affect the quality of the nanotubes [30]. To overcome this potential problem, microchannels of 5 μm in diameter have been constructed vertically throughout the suspended 50-μm-thick cantilever platform. When the reactive gases are forced to flow through these microchannels from bottom to top as illustrated in Fig. 2d, they can be modeled as miniaturized CVD furnaces. The temperature calculations based on real experimental dimensions are illustrated in Fig. 2e. The detailed process of modeling and calculation is presented in the Supplementary data. It is noted that the cold gas is quickly warmed up and its temperature becomes stable within approximately the first 5 μm into the microchannel, much shorter than the total length of the microchannel of 50 μm. Therefore, a uniform temperature profile is expected in the latter part of the microchannel which emulates that of a large scale CVD system to provide well-controlled growth environment for SWCNTs. The time during which the source gases stay at high temperature is also
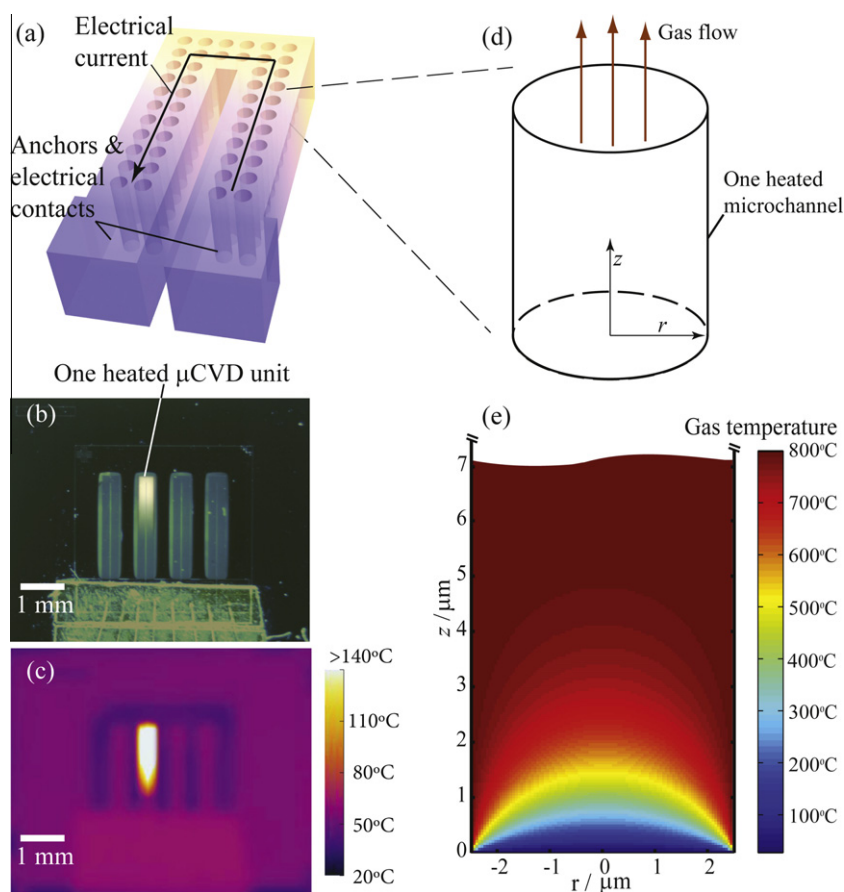
Fig. 2 – Temperature analysis of the μCVD system. (a) A μCVD unit is heated by joule heating when electrical current is applied. (b) An optical photo showing a μCVD unit is selectively heated with glowing color indicating high temperature areas. (c) Infrared image of the same structure in (b) indicating all regions but that of the heated μCVD unit are at low temperature. (d) The gas flow through one microchannel in a μCVD unit. The temperature distribution of the gas is illustrated in (e). (For interpretation of the references to colour in this figure legend, the reader is referred to the web version of this article.)

significantly shortened by the miniaturization of μCVD. This could be a problem for many CVD processes as the source gases do not have sufficient time to decompose. However this does not prominently affect the growth of SWCNTs because of the following reasons. The generally established growth mechanism for SWCNTs is the vapor–liquid–solid (VLS) process [31–34], in which carbon from the decomposed hydrocarbon gas is absorbed by the liquid-phase nanoparticle catalysts at high temperature and SWCNTs are grown as the results of the super-saturation of carbon. The gas decomposition here relies on the reaction between the catalyst and the feeding gas. So having a very short heating time is not a problem as long as the temperature is sufficiently high so that the gas molecules can have enough energy to react with the catalyst and decompose. It is noted that the formation of amorphous carbon, on the other hand, does not require catalysts and is a direct vapor–solid (VS) process. The formation of amorphous carbon is generally believed to poison the catalyst and terminate the nanotube growth [35,36]. Therefore, shortening high-temperature time by μCVD is beneficial for SWCNT growth in terms of reducing the formation of amorphous carbon [29].

2.3.　μCVD structure fabrication

In the prototype structure, the suspended cantilever is made of heavily-boron-doped (resistivity 0.005 Ω cm), single crystalline silicon. The structure is patterned (Photolithography), etched (DRIE, Deep reactive-ion etching) and released (Buffered hydrogen fluoride solution) from a SOI (Silicon-on-Insulator) wafer. It has a total length of 1750 μm, width of 300 μm and thickness of 50 μm with two anchors attached to the handling silicon layer of the SOI wafer. Backside gas openings on μCVD chip are also made by DRIE through the 550-μm-thick handling layer. A 0.5-μm-thick thermal oxide layer is grown as the barrier layer to prevent the iron nanoparticles (catalyst in SWCNT growth) from diffusing into the silicon. A photolithography is performed and the oxide on the contact pads is etched away to allow electrical contact.

2.4.　Catalyst preparation for SWCNT growth

Iron nanoparticles are deposited onto the walls of the microchannels by first dipping the whole μCVD chip into 10 mL 0.01 mM iron chloride solution. A hundred microliter 40 mM hydroxylamine hydrochloride solution is added and stirred

to help the precipitation of nanoparticles. The µCVD chip is taken out of the mixture after 20 s, rinsed and dried [37]. The chip is then heated to 800 °C for 5 min in oxygen environment in a conventional furnace. The chip is then fixed onto a chip holder, from which electrical contacts are made to the µCVD chip via wire bonding.

2.5. Growth of SWCNTs

Ethylene and hydrogen carrier gas are provided into the synthesis chamber at a volume ratio of 3:20 from the bottom. The actual mean flow velocity inside the microchannels is estimated to be 0.1 m/s by monitoring the pressure drop across the microchannels (see Supplementary data). The micro cantilever platform is heated to approximately 800 °C (the temperature distribution is estimated by a simplified electrical-thermal model [38,39]) at its center location for the synthesis of

SWCNTs under an electrical current of 180 mA and voltage of 17 V. A small aluminum heat sink is placed near the µCVD chip to provide adequate cooling. The total growth time is 10 min. It is found that the annealing of the catalyst is not necessary prior to the growth process [40].

3. Results and discussion

3.1. Characterization

As-synthesized SWCNTs have been characterized by scanning electron microscope (SEM), Raman spectroscopy, atomic force microscope (AFM), and transmission electron microscope (TEM), respectively. The SEM image in Fig. 3a shows that SWCNTs grown from the left-hand-side µCVD unit are self-aligned onto the right-hand-side silicon structure. Good alignment has been achieved as compared to the one without using
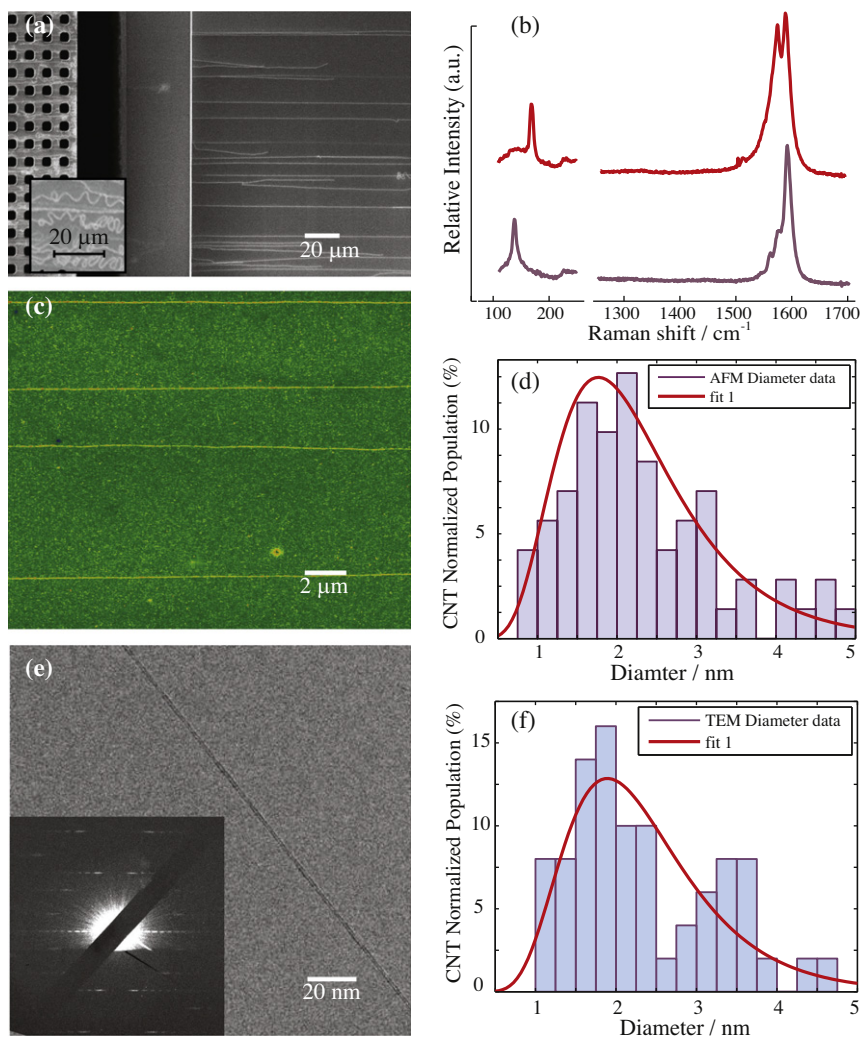

Fig. 3 – Different characterizations of the synthesized SWCNTs by µCVD. (a) SEM image showing that the nanotubes grown from the left-hand side are deposited and self-aligned on the target substrate at the right-hand side. As a comparison, the inset showed poorly aligned nanotubes without the top cap to regulate the gas flow. (b) The Raman spectral of the as-grown SWCNTs by µCVD. (c) AFM image showing four nanotubes are well-aligned on the substrate without local waviness. (d) Histogram showing the diameter distribution of the SWCNTs from 100 samples from AFM measurements. (e) TEM image of an as-grown SWCNT. The inset showed its diffraction pattern from which the chirality of the SWCNT is determined as (19, 6). (f) The histogram of the diameters of 50 nanotubes synthesized by µCVD from TEM measurements.

the top cap as illustrated in the inset of Fig. 3a. This validates the effectiveness of flow control for the alignment of SWCNTs (Supplementary data Fig. S2). The SWCNTs are free of local waviness [25] and two factors could contribute to these advancements. First, laminar flow without local turbulence is achieved as the characteristic dimension of the flow is only tens of micrometers and the Reynolds number is about 15 (Supplementary data). Similar phenomena have been reported in macro-scale CVD SWCNT synthesis by reducing reaction tube diameter and gas flow rate [24]. Second, the temperature away from the heated microchannels drops quickly to room temperature such that the possible thermal vibration [41,42] of nanotubes is minimized. The length of the SWCNTs can be controlled by the growth time. A 30-min growth produces SWCNTs with length up to ∼1 mm, while a 25 s growth results in maximum length of ∼20 μm. It is noted that growth time beyond 30 min does not give longer SWCNTs.

The Raman spectra characterization of the as-synthesized SWCNTs have been obtained using 633 nm laser at room temperature by a Renishaw® RM1000 spectrometer. Two representative Raman spectra measured at two different positions of a sample are shown in Fig. 3b with clear G mode peaks at ∼1580 cm^{-1} and no noticeable D mode at ∼1350 cm^{-1}, indicating SWCNTs with very little defects if any. The radial breathing mode (RBM) of the two spectra at 138 cm^{-1} and 169 cm^{-1} implies the diameters of the nanotubes as 1.78 nm and 1.43 nm, respectively (υ_{RBM} = 223.5 cm^{-1} nm/d + 12.5 cm^{-1} [43]). A typical AFM image with higher spatial resolution than SEM in Fig. 3c illustrates that the nanotubes remain straight and aligned. About 100 nanotubes grown by the μCVD process have been measured by AFM and the diameter histogram is shown in Fig. 3d with a mean value of 2.32 nm and standard deviation of 0.93 nm.

TEM characterizations of the synthesized SWCNTs have been obtained in a JEOL 2100 TEM operated with beam energy of 80 kV at room temperature as illustrated in Fig. 3d. Here the as-grown nanotube is suspended above the gap region of the μCVD chip (the dark strip in Fig. 3a) to allow direct TEM characterization. It appears to be very clean and the electron diffraction pattern shown as the inset helps to validate the structure as a single-walled nanotube. The nanotube in the picture is (19, 6) and its diameter is calculated to be 1.77 nm. A total of 50 SWCNTs with different diffraction patterns have been measured and the histogram of the corresponding diameter is shown in Fig. 3e. The peak probability for the diameter of the SWCNTs is at around 2 nm with mean value at 2.35 nm and standard deviation of 0.87 nm. These numbers are very close to the AFM characterizations. A total of two double-walled carbon nanotubes are found during the measurement of 56 samples. Six nanotube bundles are also found in these samples. Due to the difficulties in interpreting the electron diffraction pattern, they are not counted in the histogram. It is noted that the occurrence of nanotube bundles are closely related to the density of nanotubes. The data presented here corresponds to nanotube density of approximately 0.2/μm on the collecting substrate. In summary, the results suggest that most of the synthesized carbon nanotubes are single-walled, with little defects, and covered by little or no amorphous carbon in their pristine state.

3.2. Direct growth of SWCNTs on temperature sensitive substrates

The localized heating of the μCVD provides the possibility to place high quality SWCNTs directly onto arbitrary substrates.
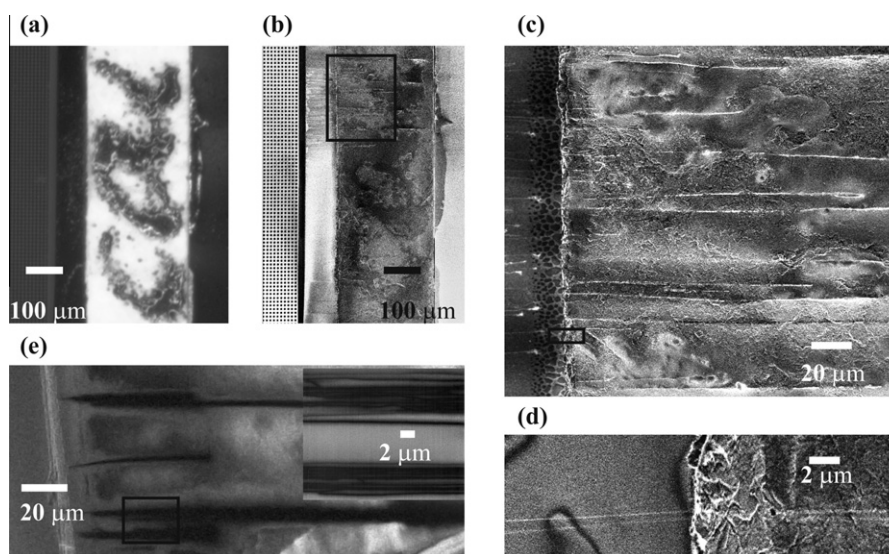

Fig. 4 – Direct growth of SWCNTs on paper and plastic substrates. (a) Optical image showing a piece of regular copy paper with letters "cal" printed by a laser printer is placed at the right side of a μCVD unit. (b) SEM picture of the same region revealing the existence of SWCNTs around the letter "l" region after synthesis. (c) SEM picture with higher magnification showing as-grown SWCNTs by μCVD deposited onto the copy paper. (d) The alignment of the SWCNTs is maintained under the influences of the surface roughness of the copy paper. (e) SWCNTs are directly deposited on a plastic tape by μCVD. The inset shows a closer SEM photo revealing that the nanotubes tend to form bundles but they do not entangle with each other on the plastic substrate.

The optical microscopic image in Fig. 4a illustrates that a piece of copy paper printed with letters "*cal*" from a laser printer is placed right next to the μCVD chip by applying a small amount of grease (Apiezon®, type H). The image is acquired after the synthesis of SWCNTs, where the piece of copy paper stays visibly intact. Fig. 4b shows the SEM image of the same area after the synthesis process, where the printed letters are still distinguishable. The close-up view around the letter "*l*" area is magnified in Fig. 4c as SWCNTs on paper are difficult to image by SEM due to electron charge effects [44]. The heating platform close to this area in the photo has the appropriate temperature for the synthesis of SWCNTs. It is observed that SWCNTs maintain good self-aligned patterns with possible obstruction from the surface roughness of the copy paper. A close-up view image is shown in Fig. 4d where two nanotubes can be identified extending from the μCVD platform from the left to the right-hand side copy paper. The two nanotubes stay close to each other with a small gap distance of less than 1 μm. The alignment is continuous without entanglement even if the shapes of the nanotubes are distorted slightly by the surface roughness of the paper. This is important because entanglement of SWCNTs will alter and degrade their electrical properties [12,13,43]. Direct growth of SWCNTs on plastic substrate (Kapton®, 2 mil tape) has also been demonstrated as illustrated in Fig. 4e. It is observed that SWCNTs tend to deposit in the bundle format without entangling with each other as illustrated in the inset of Fig. 4e. Well-aligned nanotubes can also be found on the top glass cap (which is also a low-temperature substrate, see Supplementary data) or cap made from sapphire, fused quartz, or single-crystalline quartz. All these results support the feasibility of our synthesis process. More work is underway to fabricate devices from these SWCNTs. For example, transistors can be built with this technology by simply replacing the top glass cap by an insulating substrate coated consecutively with a conductive gate electrode layer and an insulating gate dielectric layer; after the direct growth of SWCNTs onto the substrate, the transistors can be fabricated by depositing and patterning the source and drain electrodes.

4. Conclusion

In conclusion, self-aligned SWCNTs up to hundreds of microns in length have been directly grown onto various substrates including paper and plastic. The process does not involve the conventional transfer and assembly process which usually alters the properties of SWCNTs. The nanotubes are of high quality in their pristine state, and are therefore suitable for high-performance electronic applications on non-silicon, flexible, low-cost substrates.

Acknowledgements

Appendix A. Supplementary data

Supplementary data associated with this article can be found, in the online version, at doi:10.1016/j.carbon.2011.10.032.

REFERENCES

[1] Takei K, Takahashi T, Ho JC, Ko H, Gillies AG, Leu PW, et al. Nanowire active-matrix circuitry for low-voltage macroscale artificial skin. Nat Mater 2010;9(10):821–6.

[2] Zhou J, Gu YD, Fei P, Mai WJ, Gao YF, Yang RS, et al. Flexible piezotronic strain sensor. Nano Lett 2008;8(9):3035–40.

[3] Kim BJ, Jang H, Lee SK, Hong BH, Ahn JH, Cho JH. High-performance flexible graphene field effect transistors with ion gel gate dielectrics. Nano Lett 2010;10(9):3464–6.

[4] McAlpine MC, Friedman RS, Jin S, Lin KH, Wang WU, Lieber CM. High-performance nanowire electronics and photonics on glass and plastic substrates. Nano Lett 2003;3(11):1531–5.

[5] Sun D-m, Timmermans MY, Tian Y, Nasibulin AG, Kauppinen EI, Kishimoto S, et al. Flexible high-performance carbon nanotube integrated circuits. Nat Nanotechnol 2011;6:156–61.

[6] Durkop T, Getty SA, Cobas E, Fuhrer MS. Extraordinary mobility in semiconducting carbon nanotubes. Nano Lett 2004;4(1):35–9.

[7] Radosavljevic M, Lefebvre J, Johnson AT. High-field electrical transport and breakdown in bundles of single-wall carbon nanotubes. Phys Rev B 2001;64(24):241307.

[8] Yao Z, Kane CL, Dekker C. High-field electrical transport in single-wall carbon nanotubes. Phys Rev Lett 2000;84(13):2941–4.

[9] Javey A, Guo J, Wang Q, Lundstrom M, Dai HJ. Ballistic carbon nanotube field-effect transistors. Nature 2003;424(6949):654–7.

[10] Zhang ZY, Wang S, Ding L, Liang XL, Pei T, Shen J, et al. Self-aligned ballistic *n*-type single-walled carbon nanotube field-effect transistors with adjustable threshold voltage. Nano Lett 2008;8(11):3696–701.

[11] Bradley K, Gabriel JCP, Gruner G. Flexible nanotube electronics. Nano Lett 2003;3(10):1353–5.

[12] Kang SJ, Kocabas C, Ozel T, Shim M, Pimparkar N, Alam MA, et al. High-performance electronics using dense, perfectly aligned arrays of single-walled carbon nanotubes. Nat Nanotechnol 2007;2(4):230–6.

[13] Ishikawa FN, Chang HK, Ryu K, Chen PC, Badmaev A, De Arco LG, et al. Transparent electronics based on transfer printed aligned carbon nanotubes on rigid and flexible substrates. ACS Nano 2009;3(1):73–9.

[14] Ha MJ, Xia Y, Green AA, Zhang W, Renn MJ, Kim CH, et al. Printed, sub-3V digital circuits on plastic from aqueous carbon nanotube inks. ACS Nano 2010;4(8):4388–95.

[15] Burghard M, Duesberg G, Philipp G, Muster J, Roth S. Controlled adsorption of carbon nanotubes on chemically modified electrode arrays. Adv Mater 1998;10(8):584–8.

[16] Lewenstein JC, Burgin TP, Ribayrol A, Nagahara LA, Tsui RK. High-yield selective placement of carbon nanotubes on pre-patterned electrodes. Nano Lett 2002;2(5):443–6.

[17] Rao SG, Huang L, Setyawan W, Hong S. Nanotube electronics: large-scale assembly of carbon nanotubes. Nature 2003;425(6953):36–7.

[18] Lay MD, Novak JP, Snow ES. Simple route to large-scale ordered arrays of liquid-deposited carbon nanotubes. Nano Lett 2004;4(4):603–6.

[19] Meitl MA, Zhou YX, Gaur A, Jeon S, Usrey ML, Strano MS, et al. Solution casting and transfer printing single-walled carbon nanotube films. Nano Lett 2004;4(9):1643–7.

[20] Lu KL, Lago RM, Chen YK, Green MLH, Harris PJF, Tsang SC. Mechanical damage of carbon nanotubes by ultrasound. Carbon 1996;34(6):814–6.

[21] Niyogi S, Hamon MA, Perea DE, Kang CB, Zhao B, Pal SK, et al. Ultrasonic dispersions of single-walled carbon nanotubes. J Phys Chem B 2003;107(34):8799–804.

[22] Chen J, Hamon MA, Hu H, Chen YS, Rao AM, Eklund PC, et al. Solution properties of single-walled carbon nanotubes. Science 1998;282(5386):95–8.

[23] Ural A, Li YM, Dai HJ. Electric-field-aligned growth of single-walled carbon nanotubes on surfaces. Appl Phys Lett 2002;81(18):3464–6.

[24] Jin Z, Chu HB, Wang JY, Hong JX, Tan WC, Li Y. Ultralow feeding gas flow guiding growth of large-scale horizontally aligned single-walled carbon nanotube arrays. Nano Lett 2007;7(7):2073–9.

[25] Huang SM, Maynor B, Cai XY, Liu J. Ultralong, well-aligned single-walled carbon nanotube architectures on surfaces. Adv Mater 2003;15(19):1651–5.

[26] Han S, Liu XL, Zhou CW. Template-free directional growth of single-walled carbon nanotubes on a- and r-plane sapphire. J Am Chem Soc 2005;127(15):5294–5.

[27] Liu XL, Han S, Zhou CW. Novel nanotube-on-insulator (NOI) approach toward single-walled carbon nanotube devices. Nano Lett 2006;6(1):34–9.

[28] Patil N, Lin A, Myers ER, Ryu K, Badmaev A, Zhou CW, et al. Wafer-scale growth and transfer of aligned single-walled carbon nanotubes. IEEE T Nanotechnol 2009;8(4):498–504.

[29] Zhou Q, Lin L. Enhancing mass transport for synthesizing single-walled carbon nanotubes via micro chemical vapor deposition. J Microelectromech S 2011;20(1):9–11.

[30] Englander O, Christensen D, Lin LW. Local synthesis of silicon nanowires and carbon nanotubes on microbridges. Appl Phys Lett 2003;82(26):4797–9.

[31] Harutyunyan AR, Mora E, Tokune T, Bolton K, Rosen A, Jiang A, et al. Hidden features of the catalyst nanoparticles favorable for single-walled carbon nanotube growth. Appl Phys Lett 2007;90(16):163120.

[32] Alvarez L, Guillard T, Sauvajol JL, Flamant G, Laplaze D. Growth mechanisms and diameter evolution of single wall carbon nanotubes. Chem Phys Lett 2001;342(1–2): 7–14.

[33] Helveg S, Lopez-Cartes C, Sehested J, Hansen PL, Clausen BS, Rostrup-Nielsen JR, et al. Atomic-scale imaging of carbon nanofibre growth. Nature 2004;427(6973):426–9.

[34] Charlier JC, Iijima S. Growth mechanisms of carbon nanotubes. Top Appl Phys 2001;80:55–80.

[35] Liu HT, He J, Tang JY, Liu H, Pang P, Cao D, et al. Translocation of single-stranded DNA through single-walled carbon nanotubes. Science 2010;327(5961):64–7.

[36] Li YL, Kinloch IA, Windle AH. Direct spinning of carbon nanotube fibers from chemical vapor deposition synthesis. Science 2004;304(5668):276–8.

[37] Choi HC, Kundaria S, Wang DW, Javey A, Wang Q, Rolandi M, et al. Efficient formation of iron nanoparticle catalysts on silicon oxide by hydroxylamine for carbon nanotube synthesis and electronics. Nano Lett 2003;3(2):157–61.

[38] Kawano T, Chiamori HC, Suter M, Zhou Q, Sosnowchik BD, Lin LW. An electrothermal carbon nanotube gas sensor. Nano Lett 2007;7(12):3686–90.

[39] Lin LW, Chiao M. Electrothermal responses of lineshape microstructures. Sensor Actuat A-Phys 1996;55(1):35–41.

[40] Huang S, Woodson M, Smalley R, Liu J. Growth mechanism of oriented long single walled carbon nanotubes using "fast-heating" chemical vapor deposition process. Nano Lett 2004;4(6):1025–8.

[41] Zhang YG, Chang AL, Cao J, Wang Q, Kim W, Li YM, et al. Electric-field-directed growth of aligned single-walled carbon nanotubes. Appl Phys Lett 2001;79(19):3155–7.

[42] Krishnan A, Dujardin E, Ebbesen TW, Yianilos PN, Treacy MMJ. Young's modulus of single-walled nanotubes. Phys Rev B 1998;58(20):14013–9.

[43] Bachilo SM, Strano MS, Kittrell C, Hauge RH, Smalley RE, Weisman RB. Structure-assigned optical spectra of single-walled carbon nanotubes. Science 2002;298(5602): 2361–6.

[44] Homma Y, Suzuki S, Kobayashi Y, Nagase M, Takagi D. Mechanism of bright selective imaging of single-walled carbon nanotubes on insulators by scanning electron microscopy. Appl Phys Lett 2004;84(10):1750–2.